Pulsed Laser Ablation Synthesis of NbN_x ($0 \leq x \leq 1.3$) Thin Films

Randolph E. Treece,*[1] James S. Horwitz, Douglas B. Chrisey, Edward P. Donovan, and Syed B. Qadri

Naval Research Laboratory, Code 6674
Washington, D.C. 20375-5345

Received June 10, 1994
Revised Manuscript Received September 26, 1994

While a wide variety of materials have been grown as thin films by pulsed laser deposition (PLD),[2] the technique is most often used to deposit multicomponent oxide films,[3] including complex electronic ceramics such as ferrites,[4] ferroelectrics,[5] and the well-known high-temperature superconductors.[6] Recently, PLD also has been used to deposit metal nitrides. Films of AlN[7] and SiN_x[8] have been deposited in vacuum by ablating pressed-powder targets of the desired ceramic. Reactive PLD has been used to grow TiN from a Ti metal target in a nitrogen atmosphere.[9] Reports on the pulsed laser deposition growth of films of metastable β-C_3N_4[10,11] and c-BN[12] also have appeared. However, due to their extreme metastability, the growth of uniform, oriented crystalline films of these two technologically important nitrides remains elusive.

A long-term goal of ours is to develop PLD as a synthesis technique capable of growing films of new and metastable compounds so that the intrinsic properties of these materials can be accurately evaluated and used for the development of new technologies. To better understand the growth of nitride films by reactive PLD, we initiated investigations into the deposition of niobium nitride. The early transition metals usually can form several different, and sometimes metastable, nitride phases as the nitrogen to metal ratios are changed.[13] Phase assignment of NbN_x materials is complicated by the nonstoichiometric nature of the transition metal nitrides. The nonstoichiometries can be present as defects or vacancies on either the metal or nonmetal sublattices, or both, within a given phase.[13] NbN films have been deposited by chemical vapor deposition,[14] electrochemical synthesis,[15] and sputtering techniques.[16] In this communication, we describe how the PLD growth of several crystalline NbN_x ($0 \leq x \leq 1.3$) phases can be achieved simply by varying one growth parameter, the pressure of the reactive gas.

The NbN films were grown in a high vacuum chamber described in detail elsewhere.[17] The chamber was equipped with a cryopump and a turbomolecular pump operated at a base pressure of 5×10^{-8} Torr. A pulsed (10 Hz) KrF excimer laser beam (248 nm, 30 ns fwhm) was focused with a 50 cm focal length lens at 45° onto a rotating (30 rpm) and dithering Nb foil target at a laser fluence of ~6 J/cm^2. The input pressure of the ambient gas (N_2 with 10% H_2 added to reduce oxide formation) was maintained in a dynamic equilibrium (~10 sccm) by a solenoid-activated leak valve controlled by a capacitance manometer with the chamber under gated or throttled pumping. After washing with ethanol, the substrates were attached to the substrate heater with silver paste and held ~6 cm from the target. The substrate temperature (T_{sub}) was held at 600 °C and measured with a K-type thermocouple mounted in the substrate holder. The films (typically ~1200 Å thick) were characterized by Rutherford backscattering spectroscopy (RBS), X-ray diffraction (XRD),[18] and temperature-dependent resistivity ($R(T)$) measurements.[19] RBS was used to determine the deposited film compositions (x in NbN_x) and thicknesses with 6.2 meV He^{2+}. The error in nitrogen composition is $\sim x \pm 0.1$. While no oxygen was detected in the fits of the RBS spectra, the sensitivity of RBS to C, N, O atoms is low relative to Nb. Oxygen levels up to ~5% are undetectable by our current measurements, but at larger amounts, oxygen would be apparent in the RBS spectra. The NbN_x films also were examined by elastic recoil detection (ERD) with 2.0 MeV He^{2+} to determine the amount of hydrogen incorporation. The nitride films were found to contain 3–8% hydrogen irrespective of gas pressures.

The nitrogen content in the NbN_x films was found to increase with gas pressure (Table 1). Representative XRD patterns of the four crystalline phases are presented in Figure 1. The XRD pattern of the film deposited at a pressure of 10^{-7} Torr, labeled as Nb in

(1) National Research Council/Naval Research Laboratory Cooperative Postdoctoral Research Associate.

(2) A broad overview of the techniques used in and materials made by PLD has been presented in: *Pulsed Laser Deposition of Thin Films*; Chrisey, D. B., Hubler, G. K., Eds.; Wiley: New York, 1994.

(3) Growth of electronic ceramics by PLD is reviewed in: Horwitz, J. S.; Chrisey, D. B.; Grabowski, K. S.; Leuchtner, R. E. *Surf. Coatings Technol.* **1992**, *51*, 290.

(4) Carosella, C. A.; Chrisey, D. B.; Lubitz, P.; Horwitz, J. S.; Dorsey, P.; Seed, R.; Vittoria, C. *J. Appl. Phys.* **1992**, *71*, 5107.

(5) Chrisey, D. B.; Horwitz, J. S.; Grabowski, K. S. *Mater. Res. Soc. Proc.* **1990**, *191*, 25.

(6) Muenchausen, R. E.; Wu, X. D. *Pulsed Laser Deposition of Thin Films*; Chrisey, D. B., Hubler, G. K., Eds.; Wiley: New York, 1994.

(7) (a) Seki, K.; Xu, X.; Okabe, H.; Frye, J. M.; Halpern, J. B. *Appl. Phys. Lett.* **1992**, *60*, 2234. (b) Norton, M. G.; Kotula, P. G.; Carter, C. B. *J. Appl. Phys.* **1991**, *70*, 2871.

(8) (a) Xu, X.; Seki, K.; Chen, N.; Okabe, H.; Frye, J. M.; Halpern, J. B. *Mater. Res. Soc. Proc.* **1993**, *285*, 331. (b) Fogarassy, E.; Fuchs, C.; Slaoui, A.; De Unamuno, S.; Stoquert, J.-P.; Marine, W. *Mater. Res. Soc. Proc.* **1993**, *285*, 319.

(9) (a) Tiwari, P.; Zheleva, T.; Narayan, J. *Mater. Res. Soc. Proc.* **1993**, *285*, 349. (b) Cracium, V.; Cracium, D.; Boyd, I. W. *Mater. Sci. Eng.* **1993**, *B18*, 178.

(10) Treece, R. E.; Horwitz, J. S. Chrisey, D. B. *Mater. Res. Soc. Proc.* **1994**, *327*, 245.

(11) (a) Xiong, F.; Chang, R. P. H. *Mater. Res. Soc. Proc.* **1993**, *285*, 587. (b) Niu, C.; Lu, Y. Z.; Lieber, C. M. *Science* **1993**, *261*, 334.

(12) (a) Ballal, A. K.; Salamanca-Riba, L.; Doll, G. L.; Yaylor, C. A., II; Clarke, R. *Mater. Res. Soc. Proc.* **1993**, *285*, 513. (b) Ballal, A. K.; Salamanca-Riba, L.; Yaylor, C. A., II; Doll, G. L. *Thin Solid Films* **1993**, *224*, 46. (c) Qian, F.; Nagabushnam, V.; Singh, R. K. *Appl. Phys. Lett.* **1993**, *63*, 317.

(13) Toth, L. E. *Transition Metal Carbides and Nitrides*; Margrave, J. L., Ed.; Academic Press: New York, 1971; Refractory Materials, Vol. 7.

(14) Fix, R.; Gordon, R. G.; Hoffman, D. M. *Chem. Mater.* **1993**, *5*, 614.

(15) Wade, T.; Crooks, R. M.; Garza, E. G.; Smith, D. M.; Willis, J. O.; Coulter, J. Y. *Chem. Mater.* **1994**, *6*, 87.

(16) (a) Wolf, S. A.; Gubser, D. U.; Francavilla, T. L.; Skelton, E. F. *J. Vac. Sci. Technol.* **1981**, *18*, 253. (b) Cukauskas, E. J.; Carter, W. L.; Qadri, S. B. *J. Appl. Phys.* **1985**, *57*, 2538.

(17) Treece, R. E.; Horwitz, J. S.; Chrisey, D. B. *Mater. Res. Soc. Proc.* **1994**, *343*, 747.

(18) XRD patterns were collected using a rotating anode source and a conventional θ–2θ geometry and indexed using least-squares refinement. The preferred orientation was quantified by Γ (fwhm) for a particular (hkl) reflection and was measured by fixing 2θ at the peak maximum and scanning through θ.

(19) Resistivity versus temperature measurements were collected by four-point probe and cooled in liquid helium.

0897-4756/94/2806-2205$04.50/0

Table 1. Pressure Dependence of NbN_x Properties for Films Grown on MgO (100) and at 600 °C

gas pressure (mTorr)	$T_c(R=0)$ (K)	thin-film lattice parameter(s) (Å)	bulk lattice parameter(s)[a] (Å)	value of x in NbN_x	material deposited
2×10^{-4}	9.15	$a = 3.335(1)$[21]	$a = 3.30660(11)$[20]	0.0(1)	Nb
1	<4.2[b]	$a = 3.12(1)$[21] $c = 4.82(1)$	$a = 3.0563(2)$[22] $c = 4.9549(4)$	0.3(1)	Nb_2N
10	<4.2[b]	$a = 3.16(1)$[21] $c = 4.90(1)$	$a = 3.0563(2)$[22] $c = 4.9549(4)$	0.5(1)	Nb_2N
20	<4.2[b]	$a = 3.10(1)$[21] $c = 5.01(1)$	$a = 3.0563(2)$[22] $c = 4.9549(4)$	0.6(1)	Nb_2N
60	16.4	$a = 4.442(1)$	$a = 4.3927$[23]	1.0(1)	NbN
100	6.7	$a = 4.351(1)$	structure not verified[13]	1.3(1)	$NbN + Nb_3N_4$
200	<4.2[b]	$a = 4.343(1)$	structure not verified[13]	1.3(1)	Nb_3N_4

[a] Literature values for bulk materials. [b] Resistance does not go to zero above 4.2 K.

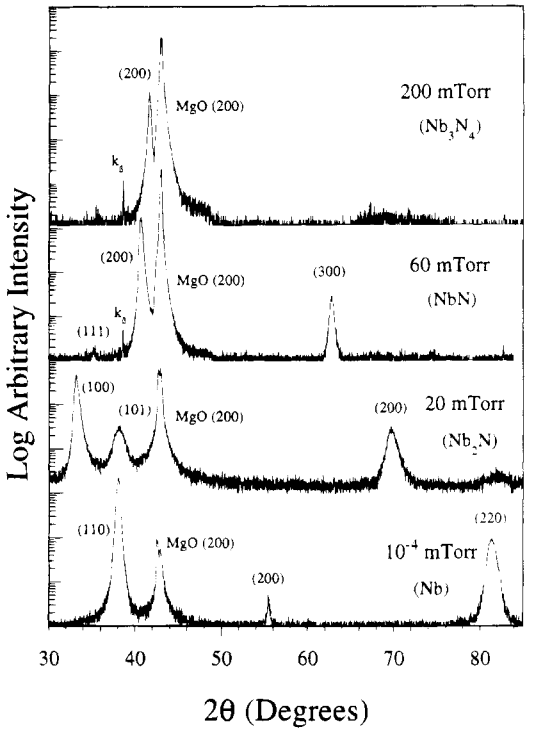

Figure 1. XRD patterns of Nb, Nb_2N, NbN, and Nb_3N_4 grown at the indicated background pressures.

Figure 1, is consistent with textured niobium[20] and was indexed with a cubic lattice parameter of $a = 3.335(1)$ Å.[21] Preferred orientation is evident in the 2θ scan, as the ratio of (220)/(200) peak intensities is larger than reported for powder samples, and the (211) reflection, expected for powders, is absent in these films. Further evidence for strong texturing can be seen by a θ scan, where $\Gamma(200) = 1.7°$ θ.

At gas pressures between 1 and 20 mTorr, the deposited films yielded XRD patterns which could be indexed as hexagonal Nb_2N with lattice constants consistent with reported values,[22] as summarized in Table 1. The film labeled Nb_2N in Figure 1, displayed strong (100) texturing and its lattice constants were calculated to be $a = 3.12(1)$ Å and $c = 4.83(1)$ Å.[21] In the films grown at these pressures, the (100) and (200) peaks are the first and second most intense reflections, respectively. In reference powder patterns, the (101) reflection is the 100% line, and the intensities of the (100) and (200) peaks are listed as <1%.[22] A peak in the θ scan of the film shown in Figure 1 revealed some preferred orientation, but less texture than observed for Nb film, with $\Gamma(100) > 3.7°$ θ. Simulations of RBS spectra revealed that the amount of nitrogen incorporated into the Nb_2N structure increased with reactive gas pressure from $x = 0.3(1)$ at a deposition pressure of 1 mTorr to $x = 0.6$ at a deposition pressure of 20 mTorr. Observation of Nb_2N phases with a range of compositions is consistent with phase diagrams of the Nb–N system where the hexagonal Nb_2N structure has been shown to be stable with $0.35 \leq x \leq 0.59$.[13]

At 60 mTorr, the XRD patterns of the deposited films readily could be identified as cubic with lattice constants $a > 4.4$ Å. The film labeled NbN in Figure 1, indexed with $a = 4.442(1)$ Å, is highly textured in (100) orientation with the substrate.[23] One measure of preferred orientation is the ratio (R) of the intensities of the (200)/(111) peaks. For the deposited NbN films, strong texturing is indicated by $R > 1000$, when compared with a randomly oriented polycrystalline NbN powder where $R = 0.86$.[23] A θ scan of the film shown in Figure 1 also indicated strong texturing with $\Gamma(200) = 1.2°$ θ. The appearance of a (300) reflection indicates that a primitive cubic distortion from the well-known rock salt NbN unit cell has occurred, leading to a new structure for NbN (described in detail elsewhere).[24] RBS spectra of films grown at 60 mTorr consistently showed compositions of $NbN_{1.0(1)}$ and ERD spectra indicated the presence of 2% hydrogen. This small amount of H does not account for the new structure of NbN observed, since, when the substrate temperature (at 60 mTorr N_2/H_2) is varied it is possible to grow NbN in the oriented rock-salt phase.[24,25] Optimization of NbN films for superconducting applications is described elsewhere.[25]

Films grown at pressures >60 mTorr displayed cubic lattice constants <4.36 Å and nitrogen compositions = $NbN_{1.3}$, as summarized in Table 1. The unit cells were determined to be cubic based on the presence of (200) and (400), as seen in the NbN films. The XRD pattern

(20) *Powder Diffraction File*; Joint Committee on Powder Diffraction Standards-International Center for Diffraction Data, Swarthmore, PA, 1986; File No. 35-789 (Nb).

(21) The a lattice parameters are expanded for the Nb (+1%) and Nb_2N (+3%) films relative to values reported for bulk samples. The thin film lattice likely is affected by the highly oriented film-substrate interface with the larger MgO substrate (a(MgO) = 4.21 Å).

(22) *Powder Diffraction File*; Joint Committee on Powder Diffraction Standards-International Center for Diffraction Data, Swarthmore, PA, 1986; File No. 39-1398 (Nb2N).

(23) *Powder Diffraction File*; Joint Committee on Powder Diffraction Standards-International Center for Diffraction Data, Swarthmore, PA, 1986; File No. 39-1155 (NbN).

(24) (a) Treece, R. E.; Osofsky, M.; Skelton, E.; Qadri, S.; Horwitz, J. S.; Chrisey, D. B. *Phys. Rev. Lett*, submitted for publication. (b) Treece, R. E.; Osofsky, M.; Skelton, E.; Qadri, S.; Horwitz, J. S.; Chrisey, D. B. *Physica C*, submitted for publication.

(25) Treece, R. E.; Horwitz, J. S.; Claassen, J. H.; Chrisey, D. B. *Appl. Phys. Lett.*, submitted for publication.

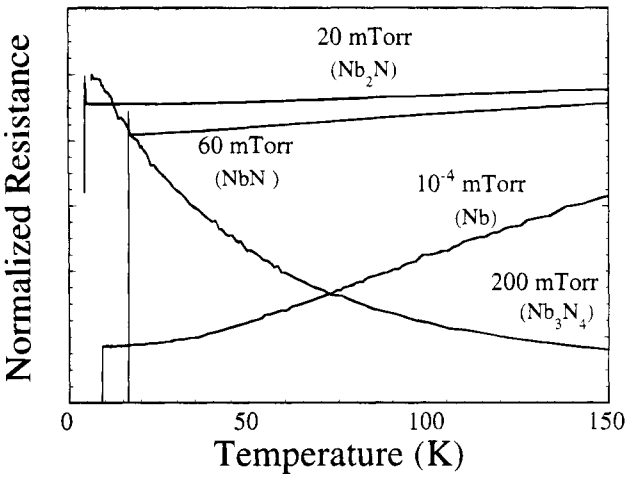

Figure 2. Normalized resistance versus temperature measurements of Nb, Nb_2N, NbN, and Nb_3N_4 deposited by PLD at the indicated background pressures.

for the highly textured NbN_x ($x \approx 1.3$) film shown in Figure 1 (labeled Nb_3N_4) is representative of the nitrogen-rich materials. This film was grown at 200 mTorr and had a = 4.343(1) Å and Γ (fwhm) = 0.8° θ, with a composition, given by RBS, of $NbN_{1.3(1)}$ and hydrogen concentration, taken from ERD, of 8%. A decrease in the lattice parameter of NbN_x with $x > 1$ is expected, since, for cubic materials with $x \approx 1$, the a's have been shown to increase with nitrogen content to a maximum when $x = 1$, and then decrease with increasing nitrogen incorporation. Bulk samples of cubic NbN_x can maintain their structure over a broad range of x values ($0.86 \leq x \leq 1.1$) by incorporating N defects when $x < 1$ and Nb vacancies when $x > 1$.[13] The highly oriented nature of these films may act to stabilize greater Nb vacancies in the rock salt structure ($x = 1.3$ for the sample grown at 100 mTorr) than has been observed in bulk samples.

In addition to differences in structure, the electrical properties of the NbN_x films also changed dramatically with composition. A plot of resistance as a function of temperature ($R(T)$) for each of the phases described above is shown in Figure 2, and the critical temperatures are listed in Table 1. The results have been normalized to allow comparison of the various measurements on the same plot. The Nb film displayed metallic behavior as it was cooled to its previously reported $T_c(R=0)$ of 9.2 K.[26] For Nb_2N, resistivity decreased with temperature slightly to an abrupt change below 5 K where there was an onset to a superconductive transition which did not go to $R = 0$ before 4.2 K. Previous investigations have noted metallic character and a lack of superconductivity above 4.2 K for Nb_2N.[16a] NbN displayed metallic behavior down to its $T_c(R=0)$ of 16.4 K. This is among the highest T_c's reported for a NbN film free of carbon impurities[27] (known to raise T_c in NbN).[16] For the nitrogen-rich films ($x > 1$), semiconducting, or activated behavior was observed with resistance increasing with decreasing temperature. The resistance of the Nb_3N_4 film grown at 100 mTorr increased as temperature was lowered to 10 K. At this point, the resistance began to decrease with temperature and dropped to zero at 6.7 K. The Nb_3N_4 film grown at 200 mTorr displayed activated $R(T)$ behavior down to 4.2 K. Both films displayed room-temperature resistivities several times higher than the other phases, consistent with properties previously reported for Nb_3N_4.[14] The low-temperature transition to superconducting behavior of the Nb_3N_4 film grown at 100 mTorr indicates that a small amount of superconductor is codeposited with the semiconducting material.

Assignment of the Nb_3N_4 phase was based on the results of all three characterization techniques (XRD, RBS, and $R(T)$). Compared to the NbN films, the Nb_3N_4 materials displayed smaller lattice constants, higher resistivities, semiconducting $R(T)$ behavior, and higher nitrogen concentrations. The totality of these results were taken as an indication that the nitrogen-rich compounds are a distinct phase, even though previous observations of Nb_3N_4 are few and the material only slightly understood.[14]

In conclusion, NbN_x ($0 \leq x \leq 1.3$) films were deposited on (100) MgO held at 600 °C by PLD of Nb foil in background of N_2 (with 10% H_2). A summary of the film composition, structure and electrical properties is presented in Table 1. The phases of the highly oriented films were assigned based on XRD, RBS, and $R(T)$. The film compositions of Nb, Nb_2N, NbN, or Nb_3N_4 have been shown to be selected easily by controlling the background gas pressure.

Acknowledgment. The authors thank Dr. C. R. Gossett for some RBS measurements, Dr. M. Osofsky for the use of his resistivity measurement apparatus, and Dr. E. F. Skelton for helpful discussions. R.E.T. gratefully acknowledges the support of the National Research Council/Naval Research Laboratory Cooperative Postdoctoral Research Associate program.

(26) Claassen, J. H.; Wolf, S. A.; Qadri, S. B.; Francavilla, T. L.; Jones, L. D. *J. Cryst. Growth* **1987**, *81*, 557. (b) Igarashi, Y.; Kanayama, M. *J. Appl. Phys.* **1985**, *57*, 849.
(27) Shoji, A.; Kiryu, S.; Kohiro, S. *Appl. Phys. Lett.* **1992**, *60*, 1624.